Electronic Supplementary Information

CO_2-crosslinked Cellulose for Radiative-cooling-driven Passive Thermoelectric Devices: One Stone Two Birds

Legeng Li[a], Doudou Xing[a], Hao Yu[a], Zhihan Wang[a], Yingjie Zhou[a,*] and Feng Yan[a,b,*]

[a] State Key Laboratory of Advanced Fiber Materials, College of Materials Science and Engineering, Donghua University, Shanghai 201620, China [b]Jiangsu Engineering Laboratory of Novel Functional Polymeric Materials, Department of Polymer Science and Engineering, College of Chemistry, Chemical, Engineering and Materials Science, Soochow University, Suzhou 215123, China

E-mail: zhouyj@dhu.edu.cn, fyan@suda.edu.cn

Experimental section

Materials

Wood pulp was supplied by Xinxiang Bailu Investment Group Co., Ltd., 1-butyl-3-methylimidazolium chloride ([BMIM][Cl], 99.0%) and 1-ethyl-3-methylimidazolium dicyanamide ([EMIm][DCA], 98.0%) was supplied by Monils Chemical Engineering Science and Technology (Shanghai) Co., Ltd., Cs_2CO_3 (99.9%, Bide) and 1,12-dibromododecane (98.0%, Adamas) were used as received.

Synthesis of the CO_2-crosslinked cellulose (Pulp-CO_2)

The wood pulp was vacuum dried at 80 ℃ for 24 h, followed by being dissolved in [BMIM][Cl] to achieve a 5 wt% cellulose solution. Then, 5.250 g of the 5 wt% cellulose solution was mixed with 1.37 g of 1,12-dibromododecane and 0.625 g of Cs_2CO_3 in a 100 mL stainless autoclave. Then, the stainless autoclave reactor was pressurized to 1.0 MPa with CO_2 and stirred at 80 ℃ for 24 h. After the reaction was completed, the stainless autoclave was cooled to room temperature, and CO_2 was gently released. The resulting mixture were washed with deionized water and ethanol for three times until Cs_2CO_3 and [BMIM][Cl] were completely removed, the obtained solid was vacuum dried overnight to obtain the CO_2-crosslinked cellulose, denoted as Pulp-CO_2. As estimated from the integral proton area of the most active C_6-OH with C_4-H as a reference from the ^{1}H NMR (**Fig. S1**), the substitution degree of the hydroxyl groups in cellulose by carbonate groups was around 5%. Increasing the amount of Cs_2CO_3 to 1.25 g could raise the substitution degree of the hydroxyl groups by carbonate groups to about 12% (denoted as Pulp-12%CO_2).

Preparation of the cellulose-based porous membranes and ionogels

A typical procedure for preparing the cellulose-based porous membranes was as follows: 1.200 g of the 5 wt% Pulp or Pulp-CO_2 dissolved in [BMIM][Cl] was dropped into a 3×3 cm^2 glass plate mold. After 2 h of indoor curing, it was immersed in deionized water every hour until [BMIM][Cl] cannot be detected. The hydrogel was vacuum dried in a freeze dryer for 48 h to obtain the porous Pulp-CO_2 membrane or Pulp membrane. To prepare the ionogels, the hydrogels were firstly placed in an ethanol bath to produce the ethanol containing gels, followed by being soaked in the mixture of [EMIm][DCA] and ethanol for 3 h. Specifically, appropriate amount of [EMIm][DCA] was mixed with 4 mL ethanol, in which the mass ration of [EMIm][DCA] to the cellulose was 0.25, 0.75, and 1.00. Finally, the gels containing [EMIm][DCA] and ethanol were vacuum dried at 50 ℃ to remove the ethanol.

Fabrication of solar thermoelectric devices

An individual radiative-cooling-driven passive thermoelectric device (RC-TED) was fabricated by coating the Pulp-CO_2 membrane (1×1 cm^2) on the Pulp-CO_2 ionogel (1×2 cm^2), with the membrane area being half that of the ionogel. The silver electrodes were attached on two sides of the ionogels. 30 individual RC-TEDs were tandemly connected, followed by being coated on the roof of a model house.

Characterizations

Scanning electron microscopic (SEM) images of the porous cellulosed-based membranes were obtained using a field emission scanning electron microscope (Regulus 8230, Hitachi,

Japan). Thermogravimetric analysis (TGA) was performed on a thermogravimetric analyzer (TG 209F3, ZETZSCH, Germany) at temperatures ranging from 40 to 800 ℃, with a heating rate of 10 ℃·min^{-1} under a nitrogen atmosphere. The Fourier-transform infrared spectra (FT-IR) in the ATR mode were collected with a Perkin-Elmer FT-IR spectrometer (PerkinElmer Spectrum Three, Germany). X-ray diffraction (XRD) patterns of the materials in the diffraction angle (2θ) range from 5 to 60° were recorded using X-ray diffractometer (D8 Advanced, Bruker, Germany). X-ray photoelectron scattering (XPS, ESCA Lab 250Xi, Thermo Fisher Scientific, USA) spectroscopy analysis was used to explore the elemental binding energy changes of ionogels. ^{1}H and ^{13}C nuclear magnetic resonance (^{1}H NMR and ^{13}C NMR) spectra of the samples were recorded on Nuclear Magnetic Resonance Spectrometer (AVANCE400, Bruker, Switzerland). The spectroscopic performance of the cellulose-based membranes was characterized separately in the ultraviolet to near-infrared (0.2–2.5 μm) using an UV–visible–near-infrared spectrophotometer (UV3600 Plus, Shimadzu, Japan) equipped with an barium sulfate integrating sphere model (ISR-603) and mid-infrared (2.5–15 μm) wavelength ranges using a Fourier transform infrared spectrometer (Nicolet IS50, Thermo Fisher Scientific, USA) with a gold integrating sphere model (IntergatIR MIR, Pike, USA). The transmission spectra (2.5–15 μm) were obtained by the Fourier transform infrared spectrometer (Nicolet IS50, Thermo Fisher Scientific, USA) equipped with a gold integrating sphere model (IntergatIR MIR, Pike, USA). Xenon lamp (oriel newport 69911, USA) was used to simulate solar illumination. The outdoor solar irradiance data was recorded using a solar irradiance tester (TES1333R, China). The temperature data was recorded through a thermocouple (DT-8891E, CEM, China). Infrared images of the samples are captured by

an infrared camera (FLIR ONE PRO, FLIR Systems, Inc.). Mechanical properties are tested using a tensile pressure testing machine (UTM2103, Shenzhen Suns Technology Stock Co., Ltd.,).

Calculation of optical data for PDRC membranes

The average solar reflectance (R_{solar}) in the full solar spectrum (0.25–2.5 μm) can be calculated using equation (S1)：

$$R_{solar} = \frac{\int_{0.3}^{2.5} I_{\mathrm{solar}}(\lambda) R(\lambda) d\lambda}{\int_{0.3}^{2.5} I_{\mathrm{solar}}(\lambda) d\lambda} \quad \text{(S1)}$$

where $I_{solar}(\lambda)$ represents the solar intensity spectrum at air mass (AM) 1.5, and $R(\lambda)$ is the spectral reflectance of a membrane.

The emissivity of the material in the atmospheric transparent window was calculated according to Kirchhoff's thermal radiation law：

$$\varepsilon_\lambda = \alpha_\lambda \quad \text{(S2)}$$

$$\alpha_\lambda + \rho_\lambda + \tau_\lambda = 1 \quad \text{(S3)}$$

Here, ε_λ and α_λ epresent the emissivity and absorption of an object under the same temperature and conditions. ρ_λ is the reflectivity, τ_λ is the ransmittance. ρ_λ was measured using an integrating sphere Fourier transform infrared spectrometer.

Thermoelectric properties of Pulp-CO_2 ionogel

The ionic conductivity (σ_i) of the ionogels were measured by electrochemical impedance spectroscopy (EIS) at an electrochemical workstation (Autolab PGSTAT302N, Switzerland) with a voltage amplitude of 100 mV in the frequency range of 1000 kHz-0.1 Hz. The ionogel was sandwiched between two stainless electrodes with an effect area of 1 cm^2, and

the ionic conductivity was determined according to the equation (S4),[S1]

$$\sigma_i = \frac{1}{R}\frac{l}{A} \quad \text{(S4)}$$

where R is the bulk resistance, l is the thickness of the ionogel, and A is the area of the ionogel.

The ionic Seebeck coefficient (S_i) was measured in a homemade temperature gradient planar configuration. Two commercial Peltier patches are used to generate temperature gradients, and the Ag wires with a diameter of 0.5 mm are used as electrodes. Two T-type thermocouples are employed to monitor the code and hot terminals of the ionogels. The generated thermal voltages were recorded on a potentiostat/galvanostat (PGSTAT302N, Metrohm, Netherlands). For outdoor experiments, the generated thermal voltages were recorded on CHI660E (CH Instruments, China). The homemade device was calibrated by measuring the polystyrene sulfonic acid (PSSH) film, which was prepared by dripping its corresponding water solution (18 wt%) onto a transparent glass substrate.[S2]

Thermal conductivities of all samples were measured by Hot Disk TPS 2500 S instrument (Hot Disk AB, Sweden) with a hot disk kapton sensor (7577 F2, radius 2 mm, the sample thickness range is no less than 2 mm) sandwiched between pairs of square samples with the dimension of 30×30 mm^2. Three independent measurements were performed on each sample with a 15 min conditioning time between each measurement. Each sample was measured independently three times, and the average of the three-test data was taken.

The ionic power factors (PF_i) of ionogel can be calculated by the Equation (S5):

$$PF_i = {S_i}^2 \sigma_i \quad \text{(S5)}$$

The ZT_i value can be calculated by the Equation (S6):

$$ZT_i = \frac{S_i^2 \sigma_i T}{\kappa} \quad \text{(S6)}$$

where S_i is the ionic Seebeck coefficient, σ_i is the ionic conductivity, κ is the thermal conductivity, and T is the absolute temperature.

Supplementary Figures

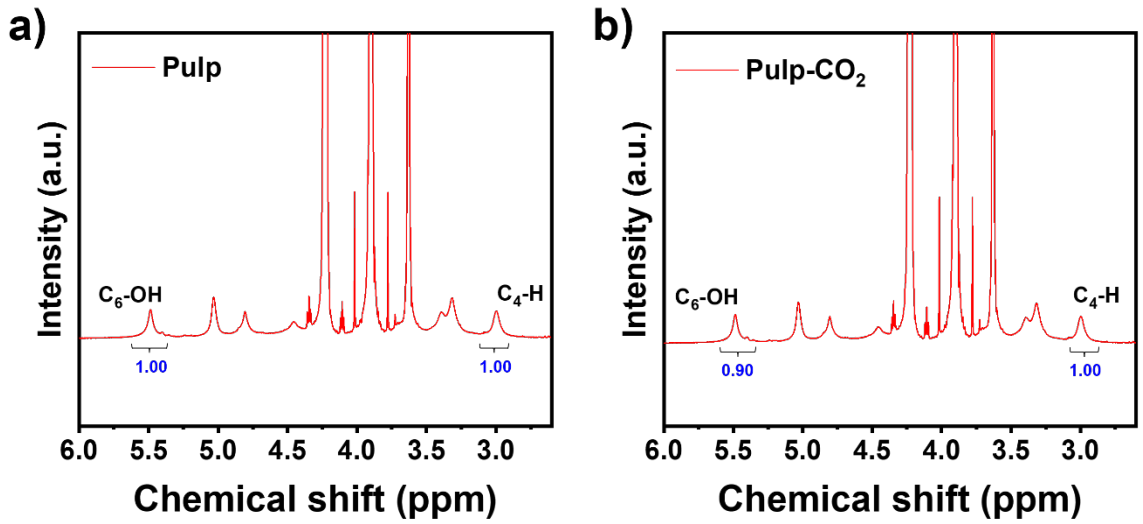

Fig. S1. ^{1}H NMR spectra of a) Pulp and b) Pulp-CO_2 with [BMIM][Cl]/DMSO-d_6 as the solvent.

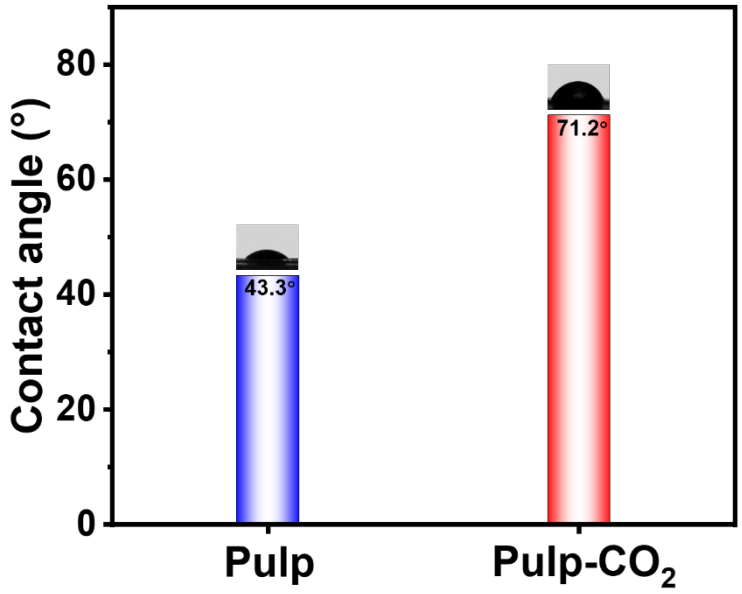

Fig. S2. Water contact angles of the Pulp and Pulp-CO_2 membranes.

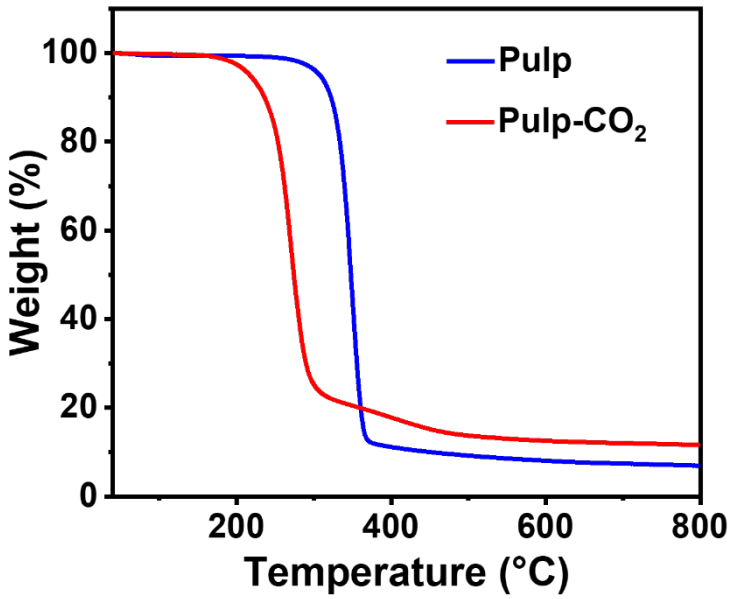

Fig. S3. Thermogravimetric analysis (TGA) curves of Pulp and Pulp-CO_2. TGA measurements were performed from 40 to 800 ℃ at a scanning rate of 10 ℃ min^{-1} under a flowing N_2 environment.

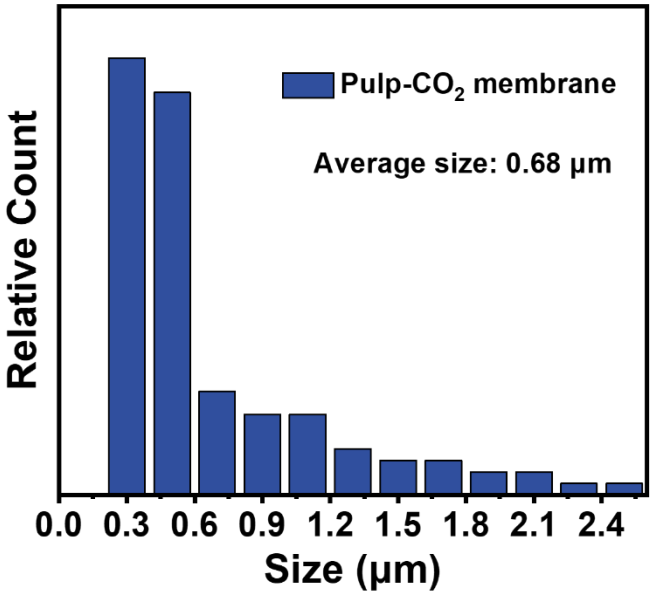

Fig. S4. Size distribution of the pores in Pulp-CO_2 membrane.

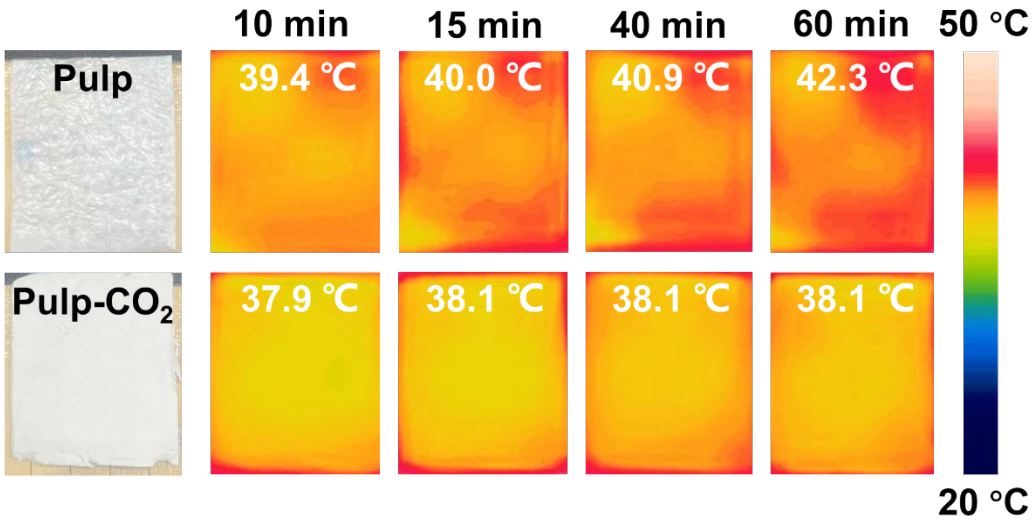

Fig. S5. Selected digital photos of the Pulp and Pulp-CO_2 membranes, and their infrared images under simulated solar irradiation within 10-60 min.

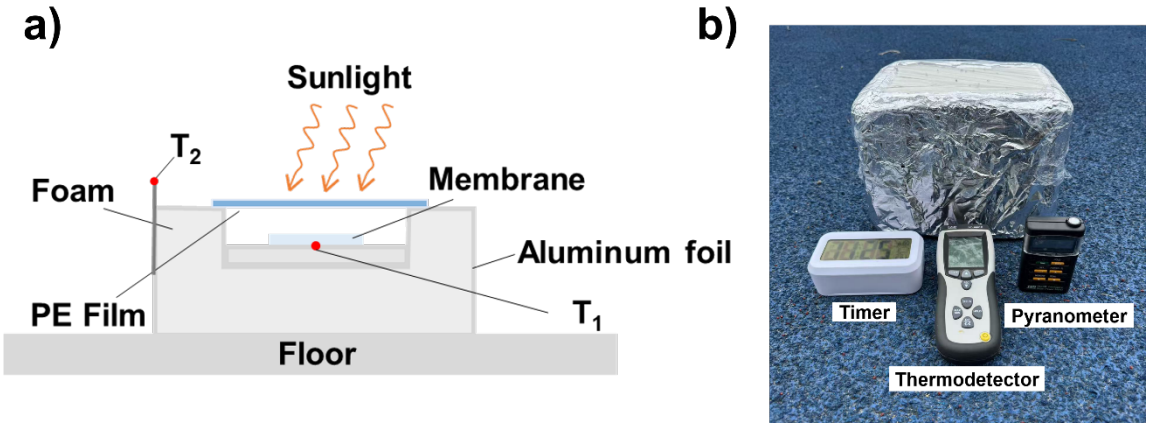

Fig. S6. a) Schematic illustration and b) digital photo of the home-made device for PDRC performance evaluation.

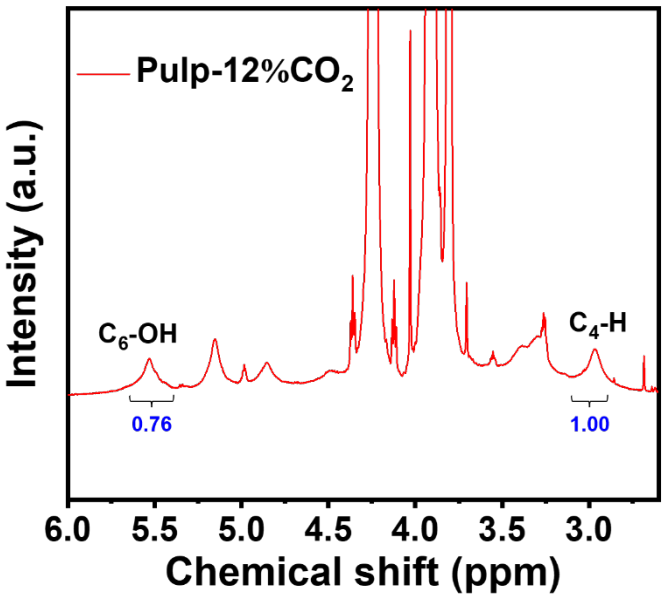

Fig. S7. ^{1}H NMR spectra of Pulp-12%CO_2 with [BMIM][Cl]/DMSO-d_6 as the solvent.

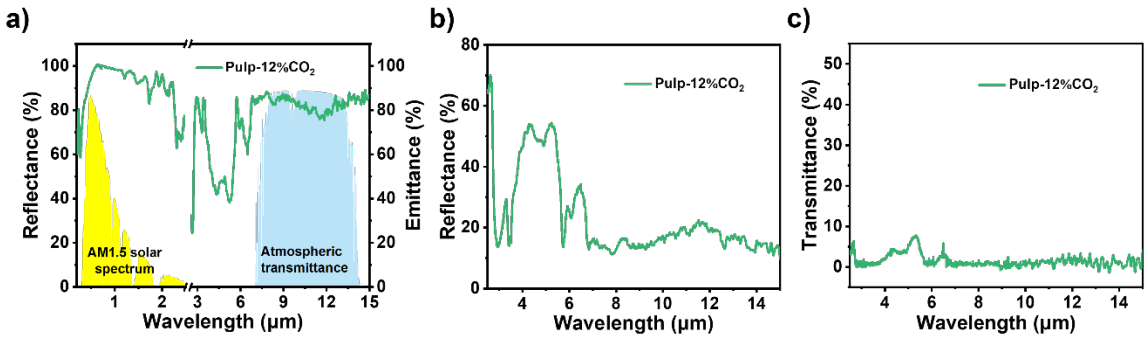

Fig. S8. a) Spectra reflective and emissivity of the Pulp-12%CO_2 membrane with 1.3 mm thickness presented against the AM1.5 solar spectrum and the atmospheric transparency window. b) Reflectivity and c) transmissivity spectra of the Pulp-12%CO_2 membrane with 1.3 mm thickness in the wavelength range of 2.5-15 μm.

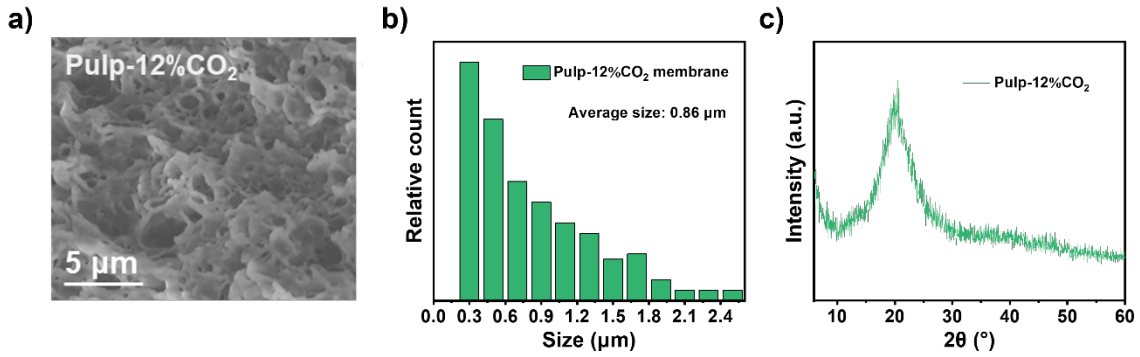

Fig. S9. a) SEM image of Pulp-12%CO_2 membrane. b) Size distributions of the pores in Pulp-12%CO_2 membrane. c) X-ray diffraction patterns of Pulp-12%CO_2.

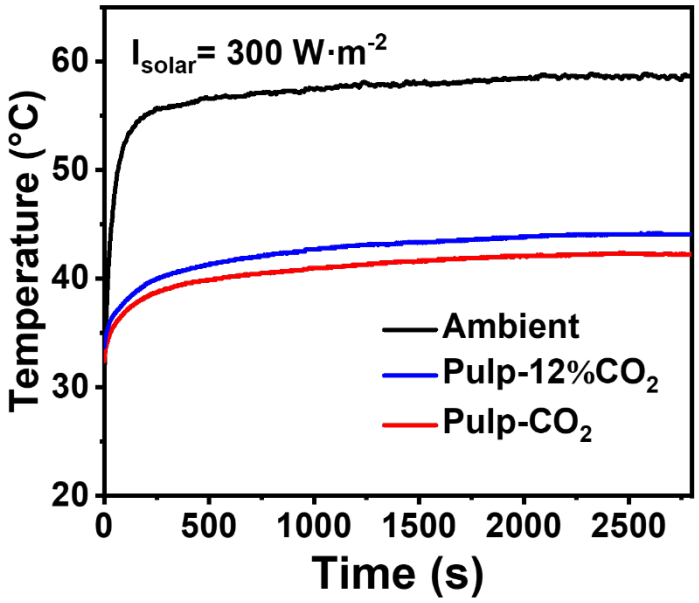

Fig. S10. Real-time temperature tracking of the ambient air, Pulp-CO_2 and Pulp-12%CO_2 membranes under simulated solar irradiance.

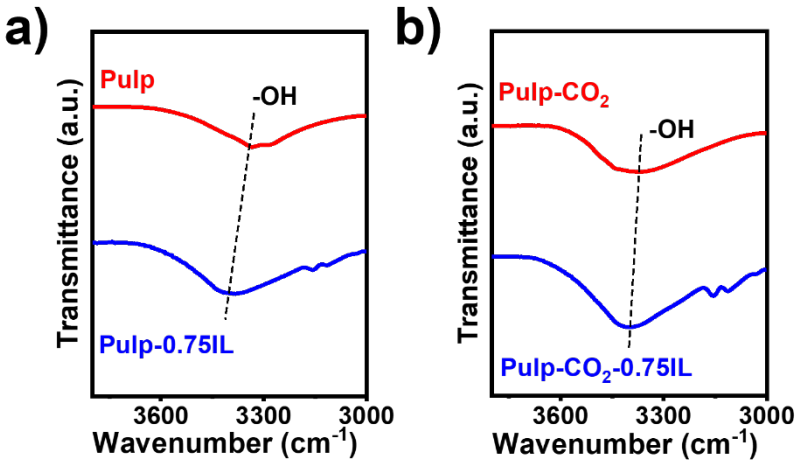

Fig. S11. FT-IR spectra of a) Pulp and Pulp-0.75IL, b) Pulp-CO_2 and Pulp-CO_2-0.75IL in the wavenumber range of 3800-3000 cm^{-1}.

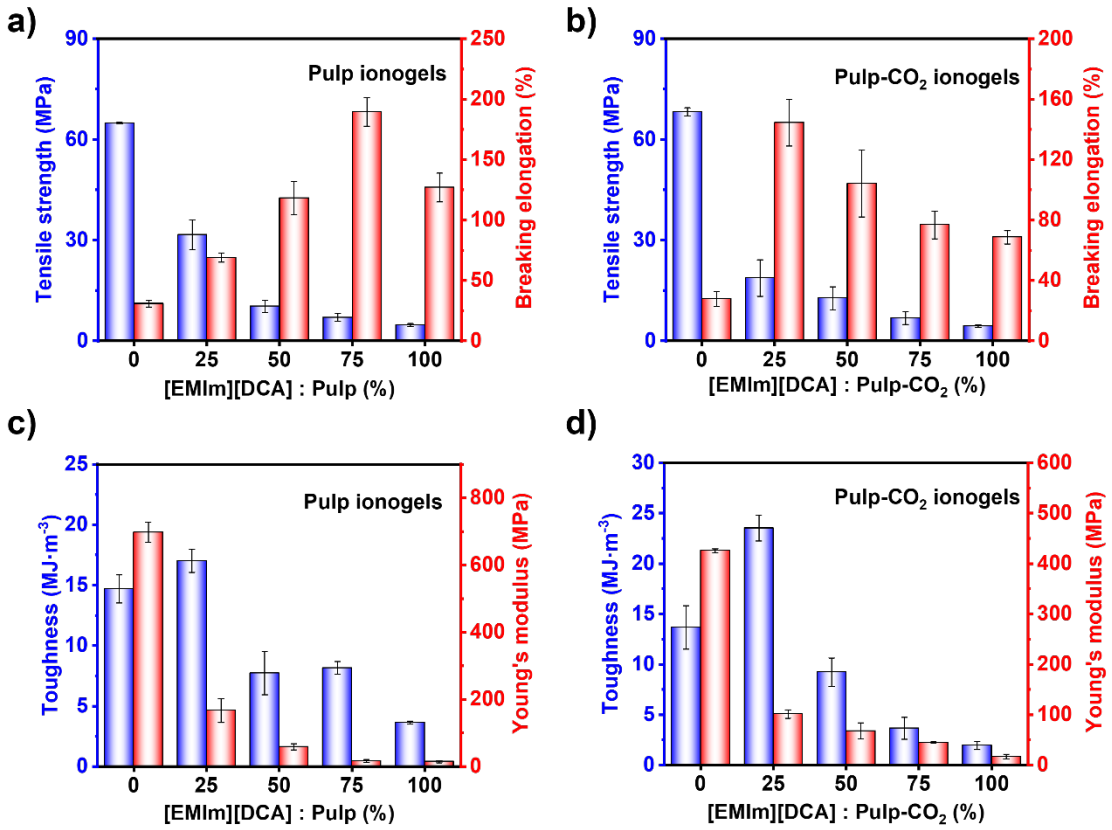

Fig. S12. Tensile strength and breaking elongation of a) Pulp ionogels and b) Pulp-CO_2 ionogels with various [EMIm][DCA] loading concentrations. Toughness and Young's modulus of c) Pulp ionogels and d) Pulp-CO_2 ionogels with different [EMIm][DCA] loading concentrations.

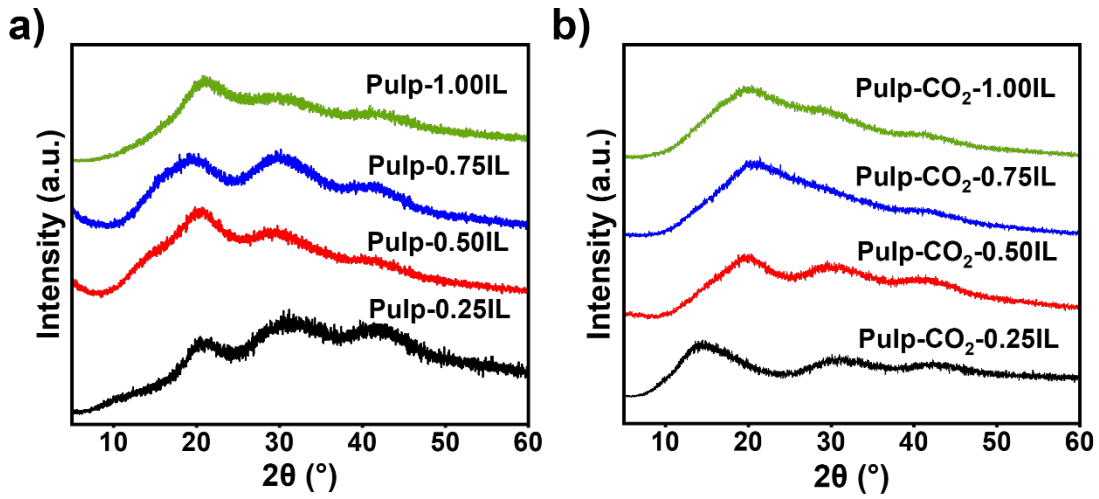

Fig. S13. X-ray diffraction patterns of a) Pulp ionogels and b) Pulp-CO_2 ionogels with different [EMIm][DCA] loading concentrations.

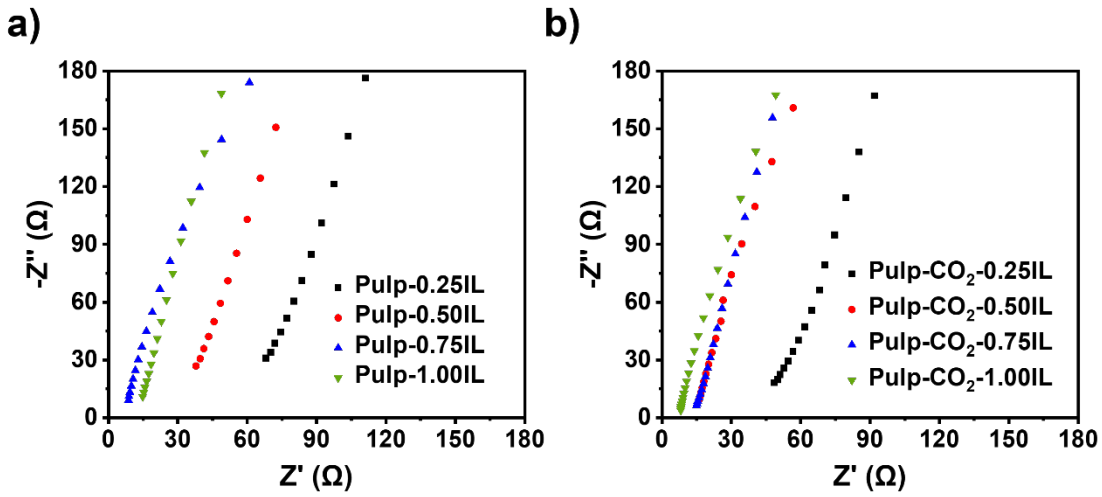

Fig. S14. Nyquist plots of the a) Pulp ionogels and b) Pulp-CO_2 ionogels with different [EMIm][DCA] loading concentrations.

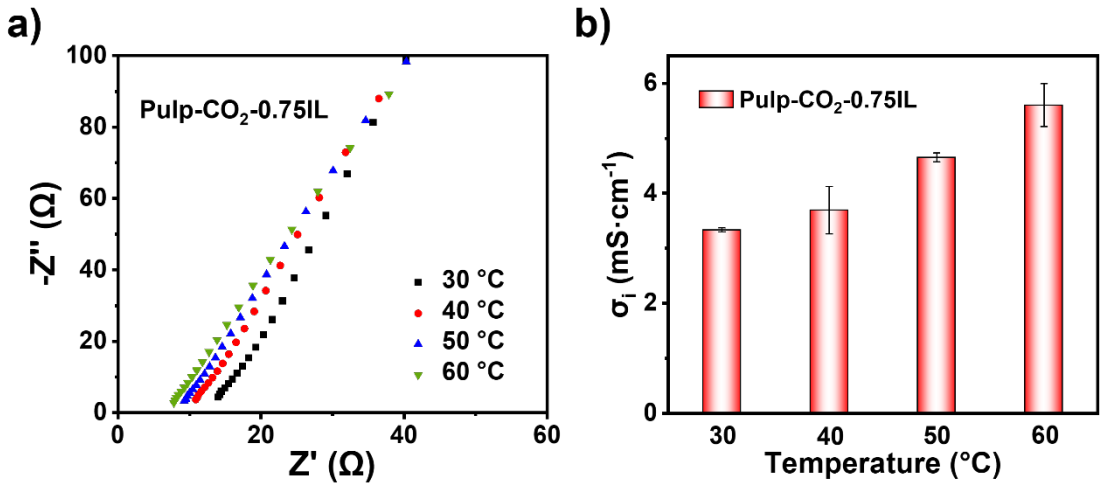

Fig. S15. a) Nyquist plots and b) ionic conductivity of the Pulp-CO_2-0.75IL at different temperatures.

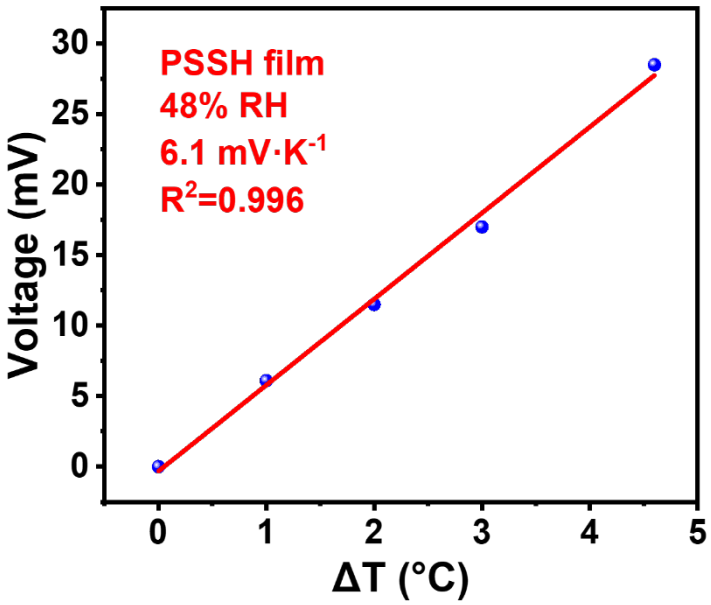

Fig. S16. Determination of the Seebeck coefficient of PSSH film (RH = 48%) for the validation of the Seebeck measurement system.

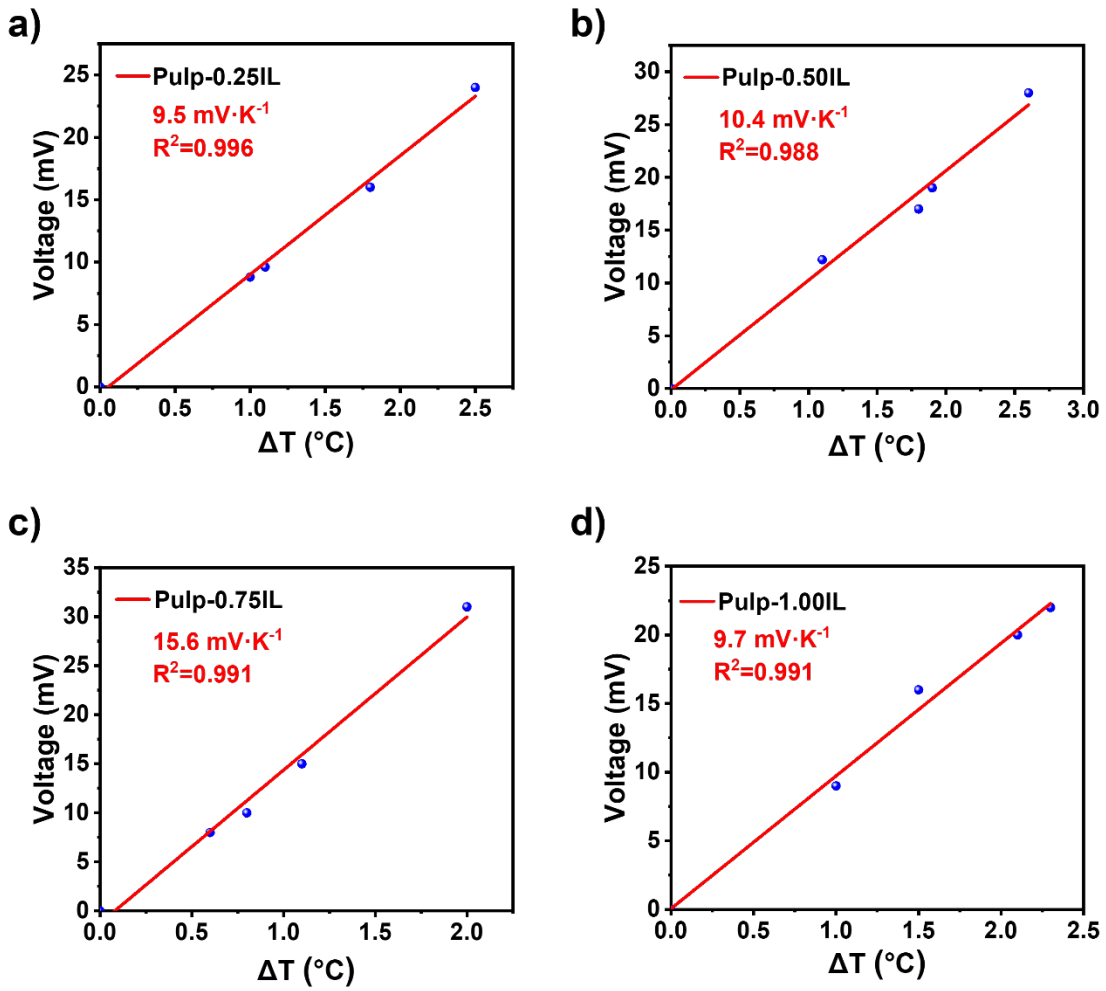

Fig. S17. Determination of the Seebeck coefficient of Pulp ionogels with different [EMIm][DCA] loading concentration of a) Pulp-0.25IL, b) Pulp-0.50IL, c) Pulp-0.75IL, and d) Pulp-1.00IL by the linear fitting of the open circuit voltage versus temperature gradient.

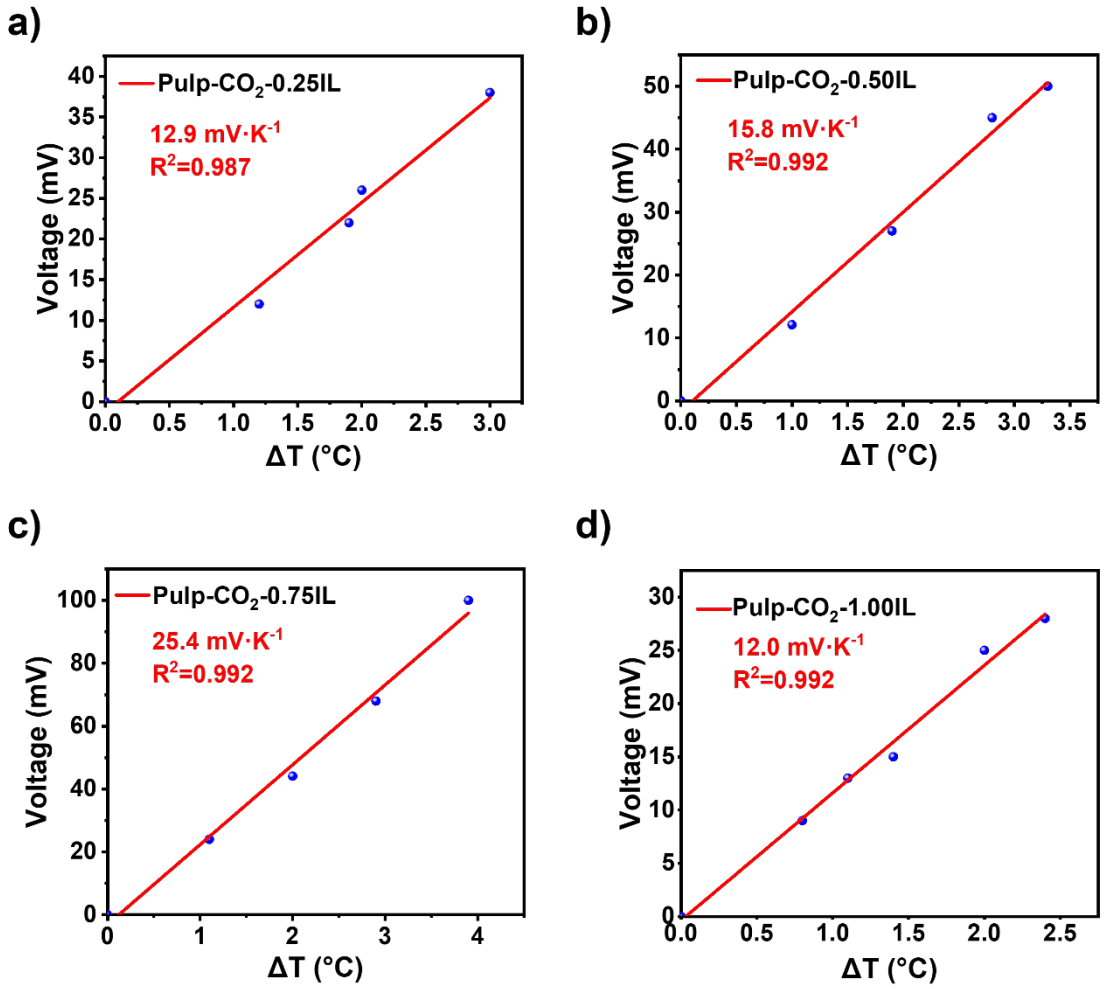

Fig. S18. Determination of the Seebeck coefficient of Pulp-CO_2 ionogels with different [EMIm][DCA] loading concentration a) Pulp-CO_2-0.25IL, b) Pulp-CO_2-0.50IL, c) Pulp-CO_2-0.75IL, and d) Pulp-CO_2-1.00IL by the linear fitting of the open circuit voltage versus temperature gradient.

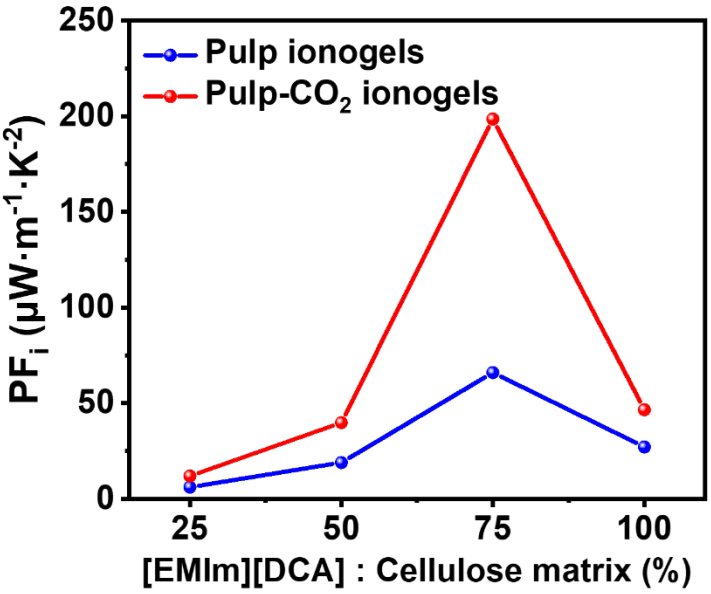

Fig. S19. Ionic power factor (PF_i) of Pulp ionogels and Pulp-CO_2 ionogels versus [EMIm][DCA] loading concentrations.

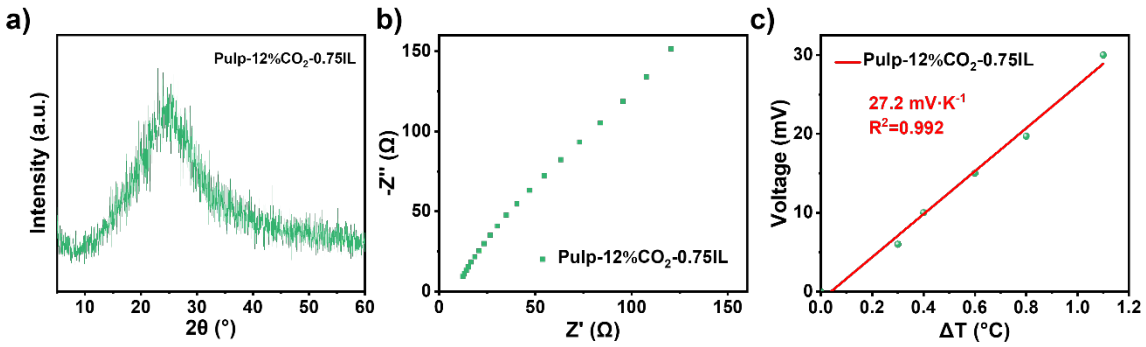

Fig. S20. a) X-ray diffraction pattern of Pulp-12%CO_2-0.75IL. b) Ionic conductivity and c) Seebeck coefficient of Pulp-12%CO_2 ionogel.

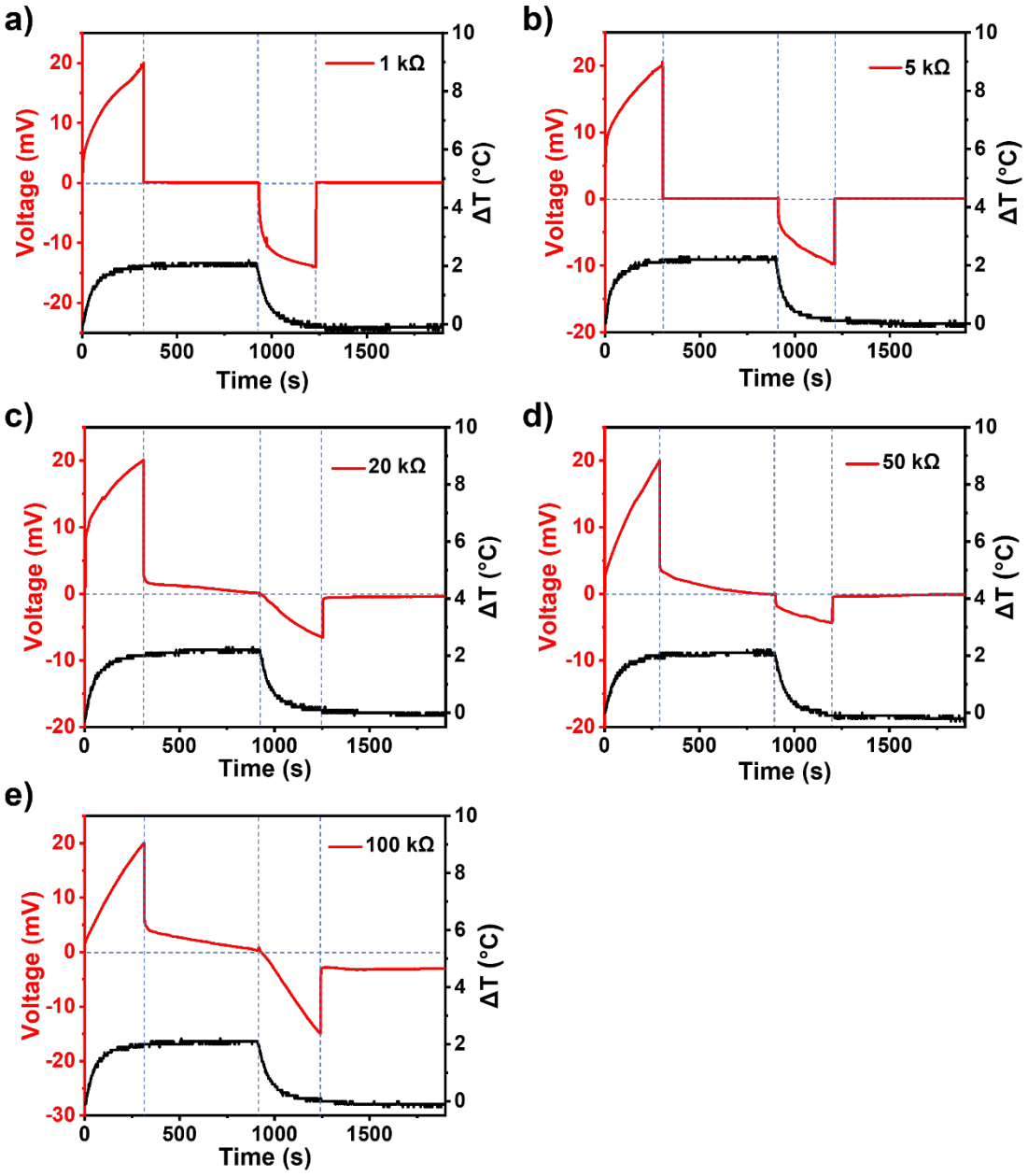

Fig. S21. Voltage profiles of the Pulp-CO_2-0.75IL-based ionic thermoelectric supercapacitor connected to an external load under a temperature gradient of 2 °C with the resistances of a) 1 kΩ, b) 5 kΩ, c) 20 kΩ, d) 50 kΩ, and e) 100 kΩ.

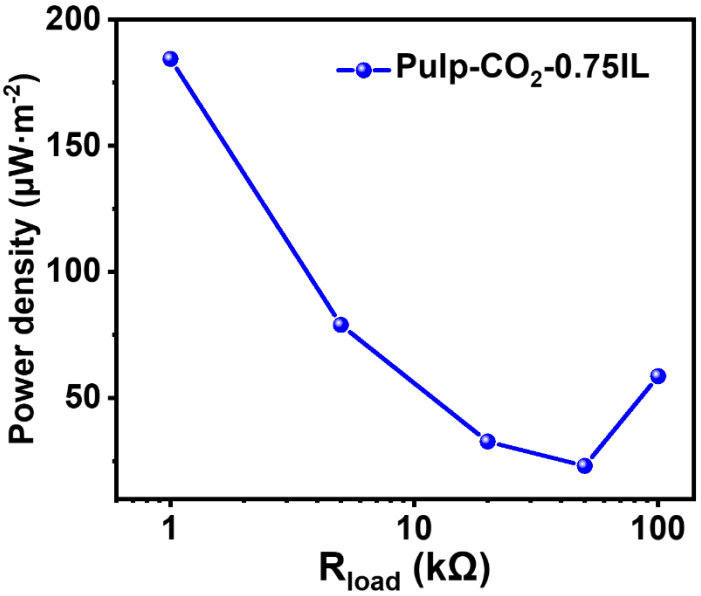

Fig. S22. Average power density supplied by the ITECs with Pulp-CO_2-0.75IL during stages II and IV on the resistance of the external load.

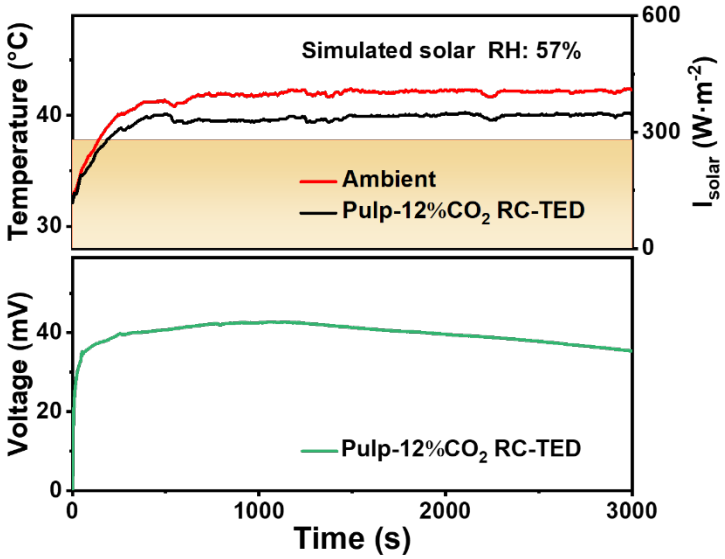

Fig. S23. Tracking of temperature gradient and output voltage of the individual Pulp-12%CO_2 RC-TED tested under simulated sunlight.

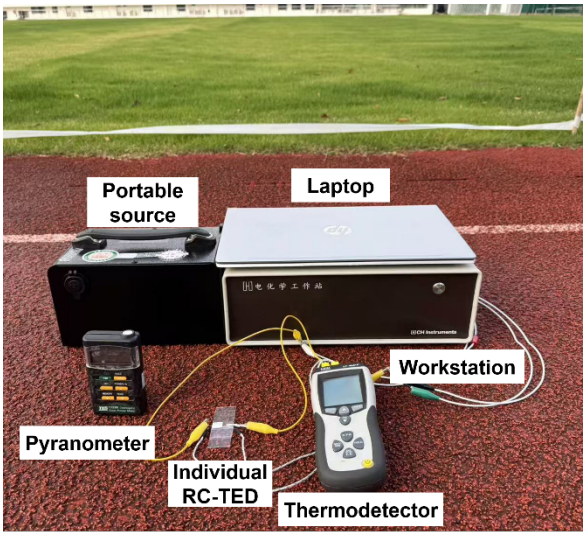

Fig. S24. Digital photo of the experimental apparatus on a playground in the campus of Donghua University (Songjiang District, Shanghai, China).

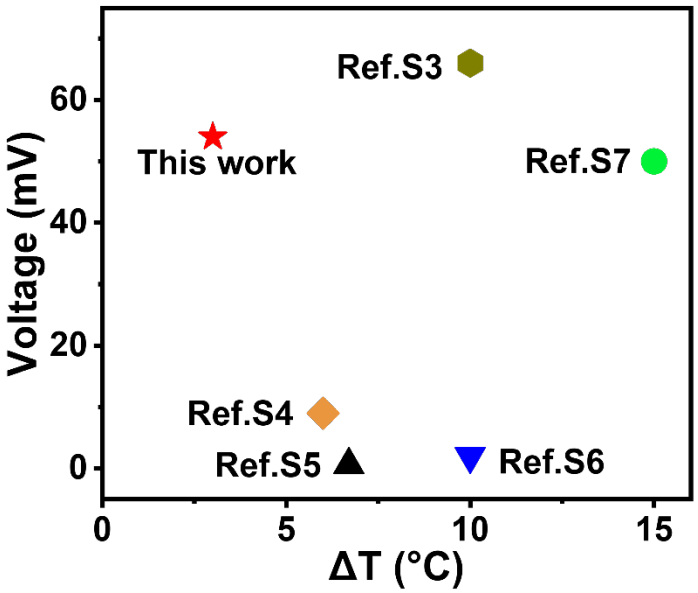

Fig. S25. Comparison of the thermovoltage and temperature gradient of the all-cellulose-based individual RC-TED and the reported representative RC-TEDs in literatures [S3-S7].

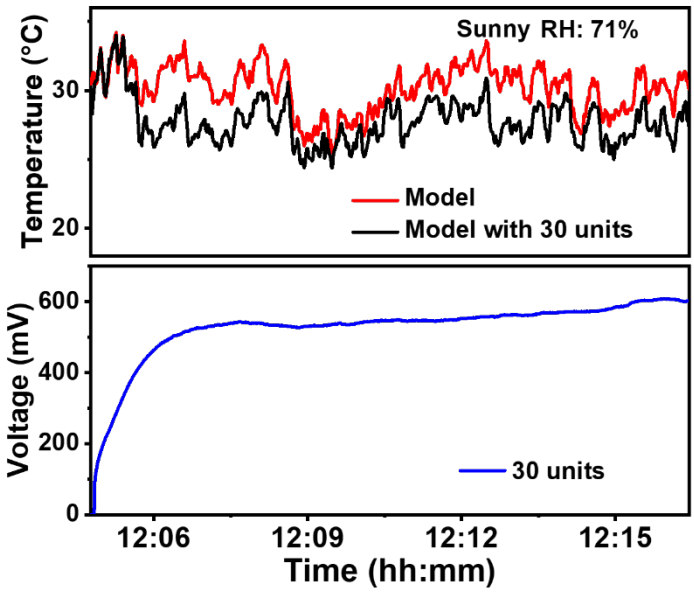

Fig. S26. Tracking of temperature gradient and output thermal voltage of 30 tandem RC-TEDs tested under outdoor environment on a sunny day in Songjiang, Shanghai (28 Nov. 2023, UTC+8).

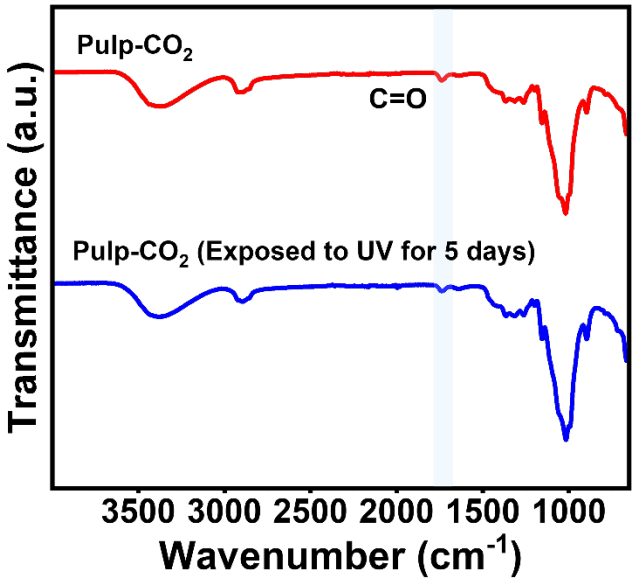

Fig. S27. FT-IR spectra of raw Pulp-CO_2 and Pulp-CO_2 exposed to UV irradiation for 5 days.

Table S1. Comparison of solar reflectance, MIR emissivity, cooling performance and thermal conductivity of Pulp-CO_2 membrane with other reported cooling materials.

Sample	Solar reflectance (%)	MIR emissivity (%)	Cooling efficiency (°C)	Thermal conductivity ($W \cdot m^{-1} \cdot K^{-1}$)	Source
Pulp-CO_2	90	91.4	12.6	0.142	This work
$SrAl_2O_4$/CNC @textiles[S8]	92	90	11.3	/	*ACS Nano*, 2025, **19**, 5029-5039.
Cellulose/SDS film [S9]	98	97	5.7	0.3	*Adv. Funct. Mater.*, 2024, **34**, 2405903.
Cellulose /PDMS fabric [S10]	90.2	98.1	6.5	/	*Chem. Eng. J.*, 2024, **489**, 151482.
CA/TiO_2 film[S11]	97.6	95	6.5	0.3	*Chem. Eng. J.*, 2023, **476**, 146668.

References

S1. Q. Li and H. Ardebili, *J. Power Sources*, 2016, **303**, 17-21.
S2. S. L. Kim, H. T. Lin and C. Yu, *Adv. Energy Mater.*, 2016, **6**, 1600546.
S3. M. Liao, D. Banerjee, T. Hallberg, C. Åkerlind, M. M. Alam, Q. Zhang, H. Kariis, D. Zhao and M. P. Jonsson, *Adv. Sci.*, 2023, **10**, 2206510.
S4. C. Chen, B. Zhao, R. Wang, Z. He, J. L. Wang, M. Hu, X. L. Li, G. Pei, J. W. Liu and S. H. Yu, *Adv. Mater.*, 2022, **34**, 2206364.
S5. C. Park, W. Lee, C. Park, S. Park, J. Lee, Y. S. Kim and Y. Yoo, *J. Energy Chem.*, 2023, **84**, 496-501.
S6. W. B. Han, S. Y. Heo, D. Kim, S. M. Yang, G. J. Ko, G. J. Lee, D. J. Kim, K. Rajaram, J. H. Lee, J. W. Shin, T. M. Jang, S. Han, H. Kang, J. H. Lim, D. Kim, S. H. Kim, Y. M. Song and S. W. Hwang, *Sci. Adv.*, 2023, **9**, eadf5883.
S7. M. Xiao, Y. Yao and W. Liu, *Sci. China Technol. Sci.*, 2023, **66**, 267-280.
S8. Y. Zhou, C. Lu and R. Xiong, *ACS Nano*, 2025, **19**, 5029-5039.
S9. C. Y. Cai, X. D. Wu, F. L. Cheng, C. X. Ding, Z. C. Wei, X. Wang and Y. Fu, *Adv. Funct. Mater.*, 2024, **34**, 2405903.
S10. S. J. Zhong, L. M. Song, W. J. Ren, W. J. Liu, S. X. Yuan, T. Q. Xu, L. Xu, J. W. Zhang, Y. Cai and L. M. Yi, *Chem. Eng. J.*, 2024, **489**, 151482.
S11. C. Y. Cai, F. L. Chen, Z. C. Wei, C. X. Ding, Y. Chen, Y. B. Wang and Y. Fu, *Chem. Eng. J.*, 2023, **476**, 146668.